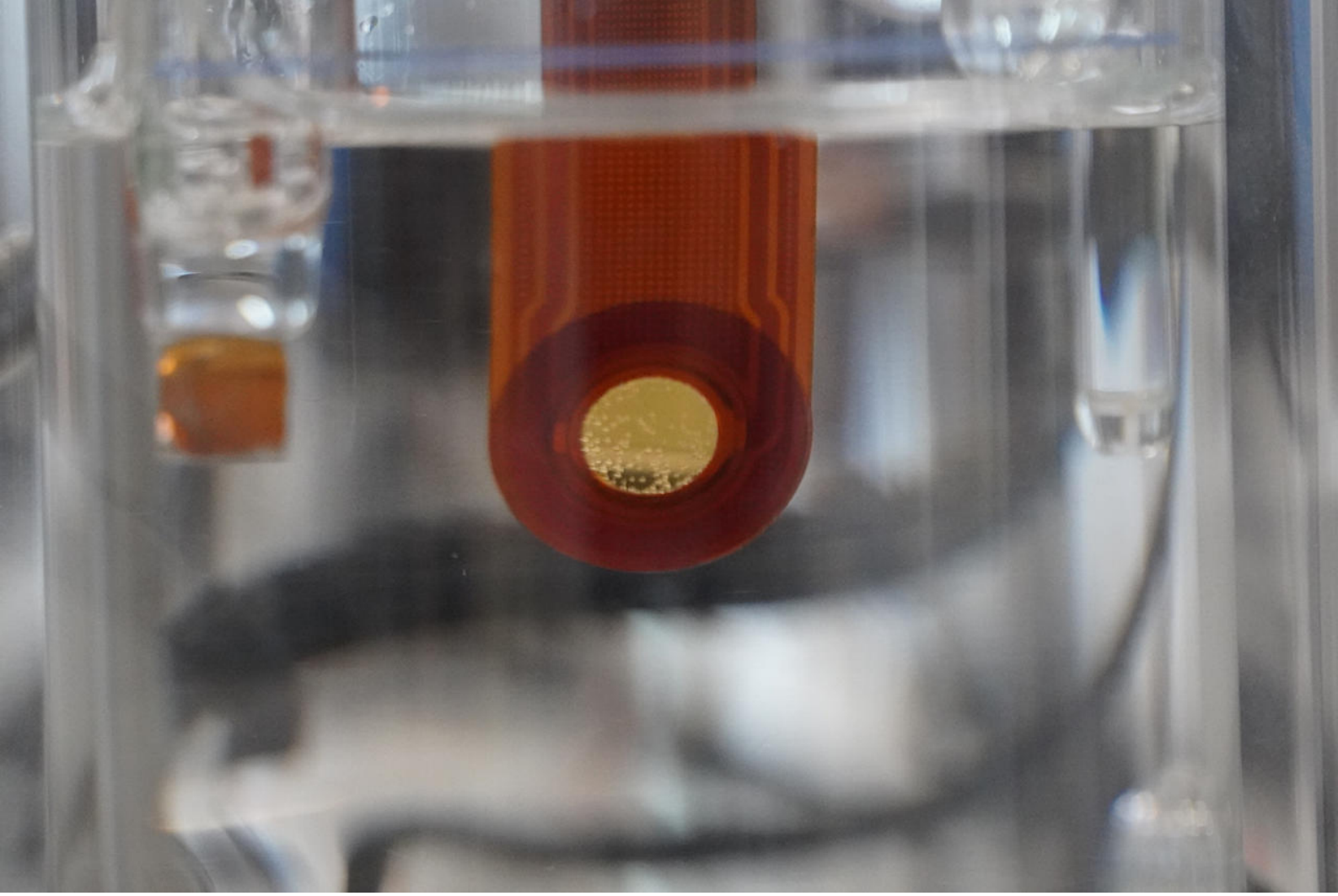


Application Note AN-EC-042

Studying zinc coatings with EQCM-D and EIS

EQCM-D with 3T analytik and Metrohm Autolab

In previous work (AN-EC-041), the eSorptionProbe, which naturally functions as the working electrode in a beaker setup, was introduced and demonstrated for electrochemical deposition and cycling studies of a battery-relevant material.

By simultaneously monitoring frequency and damping (dissipation) across the fundamental resonance and multiple overtones, this EQCM-D (electrochemical quartz crystal microbalance with dissipation monitoring) platform enables detailed characterization of soft, viscoelastic layer formation in combination with electrochemical measurements, including EIS (electrochemical impedance spectroscopy). Corrosion was also presented as an additional application area for EQCM-D.

Building on these capabilities, the present study extends the use of the eSorptionProbe to the electrochemical deposition of zinc. In this Application Note, the same system is applied to the deposition and study of Zn coatings in the presence and absence of a common additive, polyethylene glycol (PEG).

INTRODUCTION

Zinc coatings are industrially relevant to protect steel against corrosion. As a biocompatible element which is already present in the human body, it is particularly relevant in the coating of medical equipment and implants for human use [1].
Electrodeposition is the most common way to prepare high-quality Zn coatings on metal substrates. The electrodeposition can be controlled to some degree not just by the electrochemical parameters but also by additives present in the electrolyte. These additives are designed to improve the final morphological properties of the coating for the required application.

SAMPLE AND EXPERIMENTAL DETAILS

The potentiostat/galvanostat used for this study was a Metrohm Autolab AUT204 equipped with FRA32M module. The EQCM-D system was a 3T analytik eSorptionProbe OS. The fundamental as well as several overtone frequencies can be measured with this system. The working electrode consists of a 10 MHz EQCM Au crystal encased in a plastic substrate, similar in construction to a screen-printed electrode, which can be mounted onto a probe. The probe can then be inserted into almost any standard electrochemical cell, provided there is a SGJ 14/16 aperture available. Note that care should be taken to insert the probe slowly into the electrolyte, and to not immerse the electrical contact. The software packages used were NOVA, qGraph, and qGraph Viewer for associating the QCM-D and electrochemical data.
In this experiment, two solutions were used: (A) 0.01 mol/L $ZnCl_2$ and 2.8 mol/L KCl, and (B) 0.01 mol/L $ZnCl_2$, 2.8 mol/L KCl, and 10^{-3} mol/L PEG (mw ~6000). The following measurements were made on each solution: cyclic voltammetry (CV), chronoamperometry (CA), and electrochemical impedance spectroscopy (EIS). The parameters are listed in Table 1.

Table 1. Parameters used in this experiment.

Solution	A	B
Electrolyte Composition	0.01 mol/L $ZnCl_2$, 2.8 mol/L KCl	0.01 mol/L $ZnCl_2$, 2.8 mol/L KCl, and 10^{-3} mol/L PEG
Technique – CA	-1.35 V, 90 s	-1.35 and -1.8 V, 90 s
Technique – CV	Start/Stop: 0 V Upper: 0.5 V Lower: -1.8 V Scan Rate: 30 mV/s	
Technique – EIS	DC Offset: 0 V vs OCP Frequency: 100 kHz to 0.1 Hz Amplitude: 10 mV RMS	

A three-electrode cell was used consisting of the QCM Au crystal as the WE, a Pt CE, and an Ag/AgCl reference electrode.
The electrolyte was degassed with nitrogen for at

least 45 minutes prior to each measurement, and the cell headspace was continuously maintained under nitrogen. This enabled measurements to be performed in a low-oxygen environment—an important advantage, as degassing is generally not feasible in other EQCM-D setups employing static chambers or flow cells. Consequently, the eSorptionProbe OS offers a more effective means of maintaining such controlled conditions compared to conventional EQCM-D flow cell configurations.

RESULTS AND DISCUSSION

In the first instance, cyclic voltammetry was conducted using the parameters listed in Table 1. The results are shown in Figure 1.

In the case of A, on the cathodic scan a single peak is detected at -1.23 V corresponding to the uninhibited deposition of Zn^{2+} to form a layer of Zn.

On the reverse scan there is a stripping peak at -0.8 V corresponding to removal of the Zn layer. In this case, during the cycle, the deposition of the Zn is accompanied by a change in resonance frequency of about -44000 Hz, from the Sauerbrey Equation (below), corresponding to about 190,000 ng/cm^2 loaded on to the crystal.

$\Delta\phi = -C_f \cdot \Delta f$

Here, the term $C_f = 4.3$ ng $\cdot$ cm^{-2} $\cdot$ Hz^{-1} is the sensitivity coefficient for this crystal, and $\Delta\phi = \Delta m / A_q$ represents the area density. The layer thickness can then be calculated by dividing $\Delta\phi$ by the material density ρ.

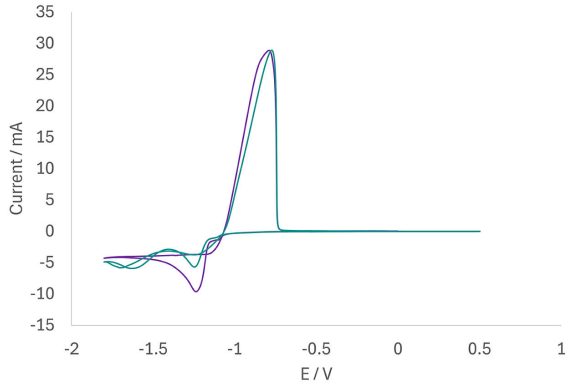


Figure 1. CVs of solutions A (purple) and B (green).

The shift in damping remains well below 10% of the corresponding frequency shift, a threshold characteristic of rigid-layer behavior to which the Sauerbrey model applies. Accordingly, considering the density of Zn, at 7.13 g cm^{-3} the layer thickness can be calculated at about 268 nm. The damping signal also allows us to estimate that one monolayer has a thickness of about 0.3 nm, due to the change in the resonance frequency of about 54 Hz, with no change in the damping signal.

In the case of B, the introduction of PEG into the electrolyte shrinks the first cathodic peak to a height that is about half of the original. Some small shift is seen, now being closer to -1.24 V. A second peak is observed at a more negative potential of -1.63 V. The stripping peak is at -0.78 V in this case. The change in the cyclic voltammogram upon the addition of PEG is also noted in the literature [2]. The new and changed features are attributed the adsorption of PEG on the surface of the electrode. The initial cathodic step is hampered by the PEG, which blocks some of the active sites – hence the lower peak height. The second cathodic step corresponds to the filling of active sites that are freed when the desorption of PEG occurs at this negative potential, as well as bulk Zn deposition.

Figure 2 shows the change in resonance frequency as a function of potential. This indicates that Zn deposition is slower in the presence of PEG, as evidenced by the reduced slope of the frequency change (green vs. purple curve).

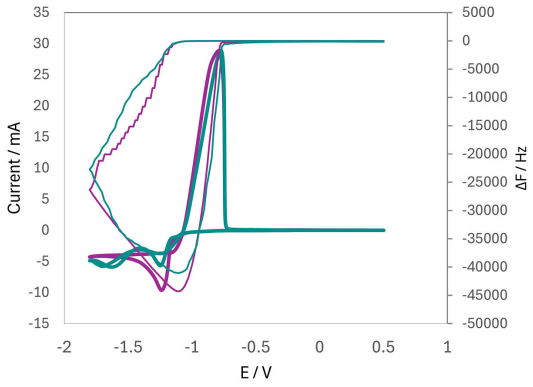


Figure 2. ΔF response during the CV in solutions A (purple) and B (green).

The change in the CV is also reflected in the damping signal, shown in Figure 3. The damping signal corresponding for the CV conducted in A shows a double peak, while in B it shows a triple peak. A double peak is consistent first with increased roughness due to the Zn deposition, through island formation, and then a subsequent fall as the islands are converted into layers, consistent with previously reported findings [3]. Regarding B, the deposition occurs in two parts. When the PEG is desorbed from the electrode in the second step, this also increases the roughness as the remaining sites are exposed, triggering a rise in the damping signal (middle peak), which then consequently falls when the Zn deposition is completed. In both cases, the last peak corresponds to the removal of Zn and cleaning of the surface.

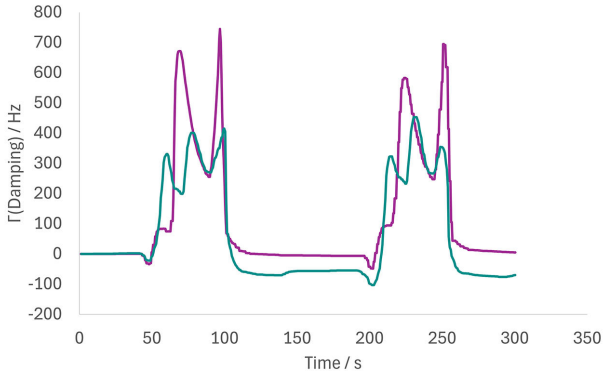


Figure 3. Damping signal during the course of the CV in A (purple) and B (green). There are two cycles shown in this figure.

Potentiostatic deposition (chronoamperometry) in conjunction with EQCM-D monitoring was also performed on solutions A and B. In the case of A, only one deposition experiment was made behind the cathodic peak, while in B, deposition was done behind both peaks in turn. See Table 1 for the details of the parameters. The results are shown in Figure 4.

Most interesting is to first consider the top green and purple curves. These correspond to A and B at the same deposition potential (-1.35 V). In the first 20 seconds of the deposition, the PEG very obviously impacts the rate of deposition as expected. The gradient is much higher without PEG than with PEG, corresponding to unrestricted PEG deposition. Eventually the gradient stabilizes and matches, which probably corresponds to bulk Zn deposition.

In Figure 4 it is also interesting to note that the deposition conducted in solution B, but at -1.8 V (bottom green curve), matches very well with the curve measured for solution A. This suggests that at this lower potential the PEG is no longer adsorbed onto the surface of the electrode, and the deposition can proceed at pace with no restriction of active sites.

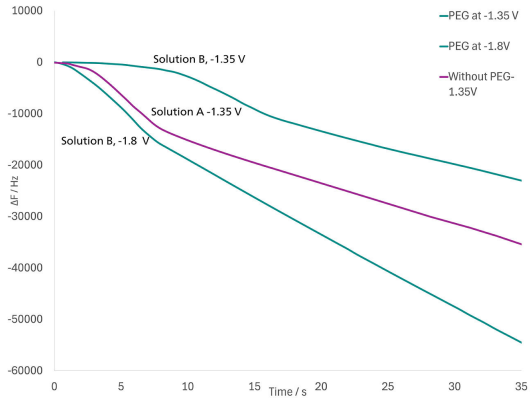


Figure 4. Deposition curves for solutions A and B, at -1.35 V and -1.8 V. For clarity, only the first ~30 seconds are shown.

EIS following the deposition was also conducted. The Nyquist plots are overlaid and shown in Figure 5. In green is the Nyquist plot recorded after the deposition in B at -1.35 V, and in purple the deposition in A at -1.35 V. Note that the spectrum recorded for A (purple), and for B at -1.8 V (black), show a much higher degree of similarity than the two plots recorded for solution B (green and black). The Nyquist plot recorded at -1.35 V in B (green) shows a larger charge-transfer reaction because the deposition is incomplete due to the blocking of PEG that leaves some of the surface exposed.

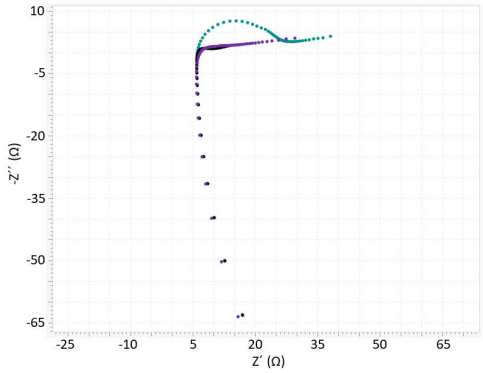


Figure 5. EIS in A and B following deposition at -1.35 V (purple and green) and -1.8 V (black).

CONCLUSION

Electrodeposition of metals for coatings is a complex process that requires considerable management of additives and parameters. This Application Note shows how EQCM-D can be used in conjunction with traditional electrochemical techniques as a powerful tool for further investigating deposition mechanisms and helping researchers optimize the process. PEG is a known electrodeposition additive which is supposed to act to slow down the reaction and produce a smoother surface. Here it is proven that this is indeed the case using EQCM-D.

REFERENCES

1. Tamurejo-Alonso, P.; González-Martín, M. L.; Pacha-Olivenza, M. Á. Electrodeposited Zinc Coatings for Biomedical Application: Morphology, Corrosion and Biological Behaviour. *Materials (Basel)* **2023**, *16* (17), 5985. DOI:10.3390/ma16175985
2. Ballesteros, J. C.; Díaz-Arista, P.; Meas, Y.; et al. Zinc Electrodeposition in the Presence of Polyethylene Glycol 20000. *Electrochimica Acta* **2007**, *52* (11), 3686–3696. DOI:10.1016/j.electacta.2006.10.042
3. Vanoppen, V.; Johannsmann, D.; Hou, X.; et al. Exploring Metal Electroplating for Energy Storage by Quartz Crystal Microbalance: A Review. *Advanced Sensor Research* **2024**, *3* (9), 2400025. DOI:10.1002/adsr.202400025

CONTACT

Metrohm SA
1 Bridle Close
2052 Woodmead
sales@metrohm.co.za

CONFIGURATION



Autolab PGSTAT204

The PGSTAT204 combines the small footprint with a modular design. The instrument includes a base potentiostat/galvanostat with a compliance voltage of 20 V and a maximum current of 400 mA or 10 A in combination with the BOOSTER10A. The potentiostat can be expanded at any time with one additional module, for example the FRA32M electrochemical impedance spectroscopy (EIS) module.

The PGSTAT204 is an affordable instrument which can be located anywhere in the lab. Analog and digital inputs/outputs are available to control Autolab accessories and external devices are available. The PGSTAT204 includes a built-in analog integrator. In combination with the powerful NOVA software it can be used for most of the standard electrochemical techniques.